J Mater Sci (2022) 57:8113–8126

Composites & nanocomposites

Adaptive VAlCN-Ag composite and VAlCN/VN-Ag multilayer coatings intended for applications at elevated temperature

Qun Cai[1,2,3], Xuebing Bai[1,2], and Jibin Pu[2,*]

[1] School of Materials Science and Engineering, Southeast University, Nanjing 211189, China
[2] Key Laboratory of Marine Materials and Related Technologies, Zhejiang Key Laboratory of Marine Materials and Protective Technologies, Ningbo Institute of Materials Technology and Engineering, Chinese Academy of Sciences, Ningbo 315201, Zhejiang, China
[3] Faculty of Mechanical Engineering and Mechanics, Ningbo University, Ningbo 315201, Zhejiang, China

Received: 23 December 2021
Accepted: 25 March 2022
Published online: 21 April 2022

ABSTRACT

High-temperature adaptive solid lubricant coatings, which could provide lubricating performance at broad temperature, are nowadays commercially available and increasingly required for industrial applications. In this work, VAlCN-Ag nanocomposite and VAlCN/VN-Ag multilayer coatings were prepared on Inconel 718 alloy by multi-arc ion planting technique of V and Ag targets either in a gaseous mixture. The multilayer coatings have a relatively higher hardness of 27 Gpa and modulus of 370 Gpa than VAlCN-Ag coatings. The toughness was significantly improved with the high H^3/E^2 of 0.147. The tribological properties were evaluated by a UMT high-temperature friction and wear tester when tested in the temperature range 25–600 °C. A positive correlation between wear rate and temperature was found for both composite and multilayer coatings. The synergistic lubricant effect derived from both $AgVO_3$ and V_2O_5 Magnéli phases is responsible for the lowest friction coefficient of about 0.18 for VAlCN-Ag coating at 600 °C. The VAlCN/VN-Ag multilayer coatings have also a low friction coefficient of 0.25, together with low wear rate of 3.2×10^{-5} mm^3/Nm, providing guidance for coating design and potential industrial applications as protective coating under high temperatures.

Introduction

Over the past decades, enormous efforts have been dedicated to improving energy transmission efficiencies with reduced coefficient of friction (COF) and extending component life spans with reduced wear rates in aviation industry application. Seeking new and effective lubricanting materials at high temperatures ($T > 500$ °C) has been a challenge for the tribology community [1–4]. Due to evaporation, decomposition and coking, traditional oil or grease

Handling Editor: Maude Jimenez.

Address correspondence to E-mail: pujibin@nimte.ac.cn

https://doi.org/10.1007/s10853-022-07153-4

lubricants fail to provide reliable lubrication under these conditions [5, 6]. Coatings prepared by plasma-spray technology or physical vapor depositions (PVD) have been widely applied on various surfaces to increase their wear resistance in extreme environments [7, 8].

Early studies showed that plasma-sprayed (PS100-400) coatings by NASA obtained low COF and achieved continuous lubrication owing to the cooperation of solid lubricants silver and alkaline halides (BaF_2/CaF_2) [9, 10]. The idea "synergistic lubrication" was firstly put forward to guide for coating design. Noting that the PS coatings with high porosity, high surface roughness and poor wear resistance cannot be widely used with great limitations in aviation. Voevodin et al. reported a series of adaptive composites including $WC/DLC/WS_2$ [5], $YSZ/Au/MoS_2/DLC$ [11], and $Al_2O_3/Au/MoS_2/DLC$ [12]. These composite coatings can maintain low COF and wear rate at medium–low temperatures. However, deteriorated mechanical strength and insufficient lubricity at high temperatures do not allow them to work above 500 °C.

Transition-metal (TM) nitrides, which exhibit high hardness, good thermal stability, high melting points, excellent corrosion, and wear resistance, have been a hot topic as protective coatings on structural component operating in complex conditions. Particularly successful examples in the TM nitride family include TiN and CrN, which exhibit substantial tribological performance promotion [13–15]. Vanadium nitride coatings (VN) are good candidates for their more common TiN, CrN in virtue of enhanced self-lubricating ability [16, 17]. Despite high wear resistance, VN coating does not provide sufficient protection in many applications. For example, the hardness and oxidation resistance decrease rapidly when VN coating suffers sliding friction at elevated temperature [18, 19]. Doping some elements such as Ti, Mo, Cu, and Si cannot simultaneously improve the hardness and oxidation resistance of VN-based coatings [20–22]. It is found that the Al addition is beneficial to coating strength and oxidation. For instance, the hardness was steadily increased from 11 GPa for VN to > 40 GPa for the $V_{0.48}Al_{0.52}N$ coatings with a non-columnar, texture-free microstructure [23]. Although it shows excellent wear resistance and oxidation with the incorporation of aluminum, the friction coefficient is not satisfactory. Meanwhile, the toughness is still hardly improved, which lead to crack formation, propagation, and ultimately reducing the coating performance. The challenge is not only to design hard solid lubricated coatings systems which can reliably keep low friction coefficient and wear rates, but also to address poor toughness issues as sliding at high temperature. In order to mitigate these problems, adding a certain amount of silver or carbon to the coating system was proven to to be an effective approach. Mu et al. [24] researched that the hardness and fracture toughness increased when the carbon was doped into VN coatings. It was also shown that the lubrication of sp^2 C–C was contributed to the low friction coefficient at 500 °C. Wang et al. [25] reported a hard yet tough V-Al-C-N coating with low friction coefficient (< 0.4) and wear rate ($\sim 1.2 \times 10^{-16}$ m^3/Nm). He also found that the special microstructure accounted for the excellent wear resistance and good toughness of such coatings as well as the cooperative lubricating effect originated from both sp^2-riched amorphous carbon and V_2O_5 Magnéli phases during sliding friction. Many research [26–28] demonstrated that soft silver phase embedded into the creamic coatings can not only decrease the friction coefficient at high temperature but also improve the toughness. Aouadi et al. [29] have pointed out that the Ag_3VO_4 storaged in the dimples contributed to the VN/Ag coatings shows the low friction coefficient ($\sim$ 0.2) at high temperature (750 °C), but life extension is also necessary. Bondarev et al. [30] have shown that the Ag-doped VCN coatings exhibited high adhesion strength and toughness when applied load as high as 1000 N for 105 cycles during dynamic impact tests. However, it is difficult to obtain the Ag-doped coatings with high toughness without compromising hardness. Our previous works [31] have also developed a series of VN-based coatings and investigate their mechanical and tribological properties. Unfortunately, improper amount of silver into the coatings leads to a significant decrease of hardness and thus reduces the wear resistance. Therefore, regulating the content of soft silver phase becomes particularly important for tuning the coatings strength.

In addition, multilayer coating is considered as a promising approach which yields an enhancement of the coating toughness without sacrificing the strength [32–34]. There are some interfaces in the multilayer coating which can dissipate energy, inhibit columnar crystal growth and suppress crack initiation and propagation, thereby promoting the comprehensive

performance of the coatings [35]. Therefore, this work aims at regulating the content of silver by altering the number and position of targets and optimizing coating structure by establishing many interfaces to enhance tribological performance, adhesion strength, and fracture toughness of coatings. The VAlCN/Ag composite and VAlCN/VN-Ag multilayer coatings were designed and prepared by multi-arc ion plating system. The relationship among the coating structure, mechanical properties and tribiological behavior was discussed.

Coating deposition

The VAlCN-Ag composite and VAlCN/VN-Ag multilayer coatings were prepared on Inconel 718 alloy and silicon substrates by multi-arc ion plating techniques (Hauzer Flexicoat 850) using V (purity 99.99 at%) targets, Al (purity 99.95 at%) targets, and Ag (purity 99.9 at%) targets. Due to the limitation of graphite target in multi-arc ion plating system, acetylene was use as the carbon source. Prior to loading into the chamber, the substrates were completely cleaned in acetone and alcohol for 15 min, respectively, and then dried. The samples were fixed on a rotational holder, and the chamber was pumped down to a background pressure less than 4×10^{-3} Pa. Then the substrates were cleaned by Ar^+ bombardments for 2 min with negative bias voltages of − 900, − 1100 and − 1200 V to remove thin oxide layer and contaminants on the surfaces. One Ag target was used for VAlCN-Ag coatings, and two Ag targets were utilized for VAlCN/VN-Ag coatings. A VN buffer layer was first deposited for 6 min with V targets current of 60 A and substrate bias of − 50 V in the mixed atmosphere of Ar and N_2 to enhance the adhesion of VAlCN-Ag and VAlCN/VN-Ag coatings on the substrates. Then, both coatings were deposited for 70 min. The specific deposition process parameters are as follows: the V, Al, and Ag targets currents of 60, 32, and 35 A, the deposition temperature of 350 °C, the bias voltage of − 70 V, the N_2 (purity 99.99%) flow rate of 350 sccm, and the C_2H_2 (purity 99.99%) flow rate of 60 sccm. The multilayer coatings were deposited by rotating the substrate with a speed of 2 rpm and controlling the opening time of shutter with 5 min for the VN-Ag individual layer, 4 min for VAlCN individual layer, and 2 min for top VAlCN layer.

Characterization and mechanical tests

The surface and cross-sectional images of as-deposited coatings were investigated by scanning electron microscope (FEI, Verios G4 UC) and field emission scanning electron microscope (Hitachi, S4800), respectively. The chemical composition of the coatings was detected from the elemental depth profiles measured by a GDA-750 Glow Discharge Optical Emission Spectrometer (GDOES, Spectruma Analytik GmbH, Germany). X-ray diffraction (XRD, Bruker D8 X-ray facility) with Cu Kα radiation (λ = 0.154 nm) was utilized to explore the structure and phase composition. The scanning angle ranged from 20 to 90° at a scanning speed of 4°/min with a step size of 0.02°. Meanwhile, Raman spectroscopy (Renishaw inVia Reflex, UK) was used to analyze the carbon peaks (disorder D and G peaks). The microstructure was studied in more details by TEM, high-resolution TEM (HRTEM) (Tecnai F20, USA). The results were analyzed by Digital Micrograph software. Prior to testing, the cross-sectional samples were prepared by focused ion beam (FIB, Zeiss Auriga) technique at 30 kv applied voltage for TEM. The hardness and elastic modulus of coatings were measured by a nanoindenter system with a Berkovich indenter (MTS, G200). Considering the rough surface of the coatings by arc ion plating, the samples were polished by dimple devices to surface roughness less than 50 nm before the tests. Six measurements were obtained, and the average values were employed to minimize the measure errors. The hardness and elastic modulus were calculated according to the Oliver–Pharr method from the load–displacement curves.

Tribotesting

The friction and wear behaviors of the VAlCN-Ag and VAlCN/VN-Ag coatings were investigated on a UMT-3 tribometer (CETR, USA) in ambient air at different temperatures (room temperature, 200, 400, 600 °C). The relative humidity and room temperature were about 58 ± 5% and 24 ± 2 °C, respectively. Al_2O_3 balls with a diameter of 6 mm were used as the counterparts on a frictional instrument under normal load of 5 N, linear sliding speed of 50 mm/s, and wear track diameter of 5 mm. The sliding wear tests lasted for 30 min and CoFs were continuously recorded during the sliding process. Based on the

wear track depth profiles determined by the contact profilometer (Alpha-Step IQ, USA), the wear loss could be calculated after the sliding a distance about 90 m. The average of three measurements was taken. The wear rate was defined by the formula $K = V/SF$, where V is the wear volume of coating, F is the constant normal load, and S is the sliding distance. The worn surface was observed by SEM (Hitachi S-4800, Japan). The elemental distribution in wear tracks of coatings and wear scars of balls was determined by FE-SEM (FEI Quanta FEG 250) equipped with energy-dispersive spectroscopy (EDS, OXFORDX-Max). Furthermore, the phase composition was detected by Raman after high-temperature testing.

Results and discussion

Microstructure

Figure 1 shows the surface and cross-sectional morphologies of as-deposited coatings. The surface presents dispersed microparticles of different sizes, especially that on the VAlCN/VN-Ag coating, can be observed more clearly in Fig. 1d. The microparticles are produced by unstable arc discharge on the target surface and splattered onto the coating surface during deposition [36]. Figure 1b, e depicts the cross-sectional morphologies of composite and multilayer coatings. The multilayer coating exhibits a compact structure while the composite coating presents a disordered structure with some gullies. The thickness of the coatings is 2.16 and 2.28 μm, respectively. The enlarged image in Fig. 1f presents the individual layer thickness of VAlCN/VN-Ag multilayer coating, in which the thickness of the cohesive layer is 180.0 nm, the individual VN-Ag layer is 119.0 nm, and the individual VAlCN layer is 92.8 nm. The final VAlCN layer is visibly seen upside for all the VAlCN/VN-Ag multilayer coatings.

The GDOES elemental depth profiles for VAlCN-Ag and VAlCN/VN-Ag coatings are presented in Fig. 2. The alternative individual VAlCN and VN-Ag layers can be identified by the modulation waves of Ag, Al, and C signals (Fig. 2b) compared with the monotonous variation in VAlCN-Ag composite coating with depth (Fig. 2a). However, the variation periods gradually disappear with the increase in depth. This phenomenon seems to be owing to layer inter-diffusion.

Figure 3 shows typical XRD patterns and Raman spectra of the VAlCN-Ag and VAlCN/VN-Ag coatings. The observed peaks correspond to the (111), (200), (220), and (311) planes of a single-phase VCN solid solution and Ag second phase, indicating a random orientation of the coatings. In a cubic B1 NaCl-type lattice, V and Al atoms occupy the (0, 0, 0) positions, whereas C and N atoms locate in the (1/2, 1/2, 1/2) sites. Additional information on the phase composition of the VAlCN-Ag and VAlCN/VN-Ag coatings obtained using Raman spectroscopy is given in Fig. 3b. Two divided regions in VAlCN-Ag coating can be distinguished, that is, one located between 100 cm^{-1} and 1000 cm^{-1} corresponds to the vibrational modes of (V, Al) (C, N) compounds, while the other between 1200 and 1800 cm^{-1} indicates the existence of amorphous carbon phase. The amorphous carbon spectra can be fitted into two peaks, including G peak centered at 1580 cm^{-1} from diamond-like sp^3 bonds and D peak centered at 1376 cm^{-1} due to the aromatic sp^2 bonds. Besides, Raman peaks of multilayer coating were weaker than that of the composite coating.

Figure 4 shows the high-resolution TEM images (a) with corresponding SAED of VAlCN/Ag coating. Two main lattice fringes with spacings of 0.235 and 0.238 nm are found, corresponding to Ag (111) and VCN (111), respectively. It can be seen that the two bright rings of SAED patterns correspond to the VCN (111), Ag (111), and Ag (200), respectively. Further TEM observations are given in region 1 and region 2, marked with the red box and operated by inverse Fourier filter conversion. Obvious stacking faults in region 1 indicate the irregular arrangement of atoms during deposition. Region 2 represents a polycrystalline including three growth directions, where both (111) and (200) on the left bottom belong to VCN.

Figure 5 shows the high-resolution TEM images of VAlCN/VN-Ag coating (a) with the corresponding SAED patterns. The lattice spacing of 0.235, 0.238, 0.205, and 0.209 nm is ascribed to Ag (111), VCN (111), Ag (200), and VCN (200), respectively, indicating that there are polycrystalline phases in the multilayer coating.

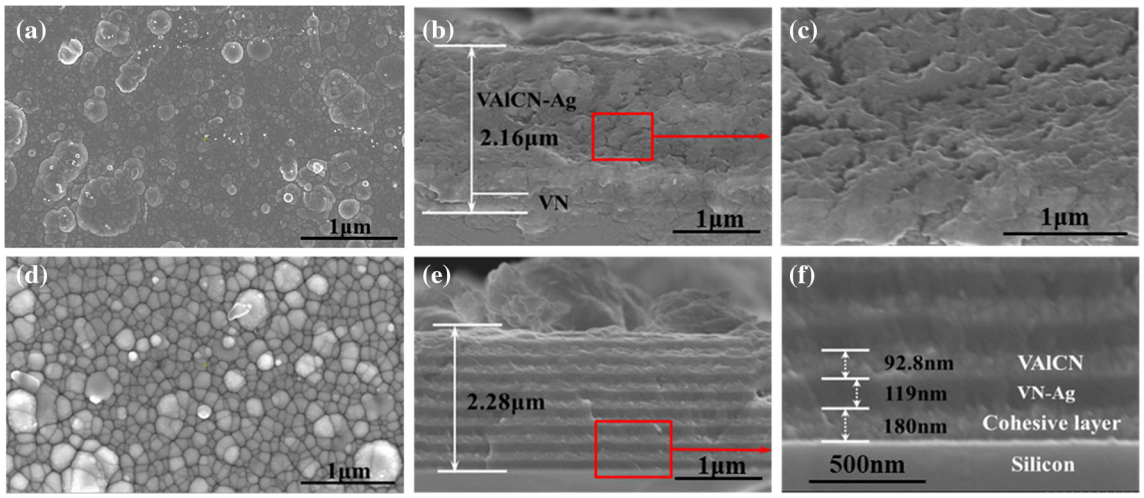

Figure 1 Surface, cross-sectional morphologies and enlarged images of VAlCN-Ag (**a**–**c**) and VAlCN/VN-Ag (**d**–**f**) coatings.

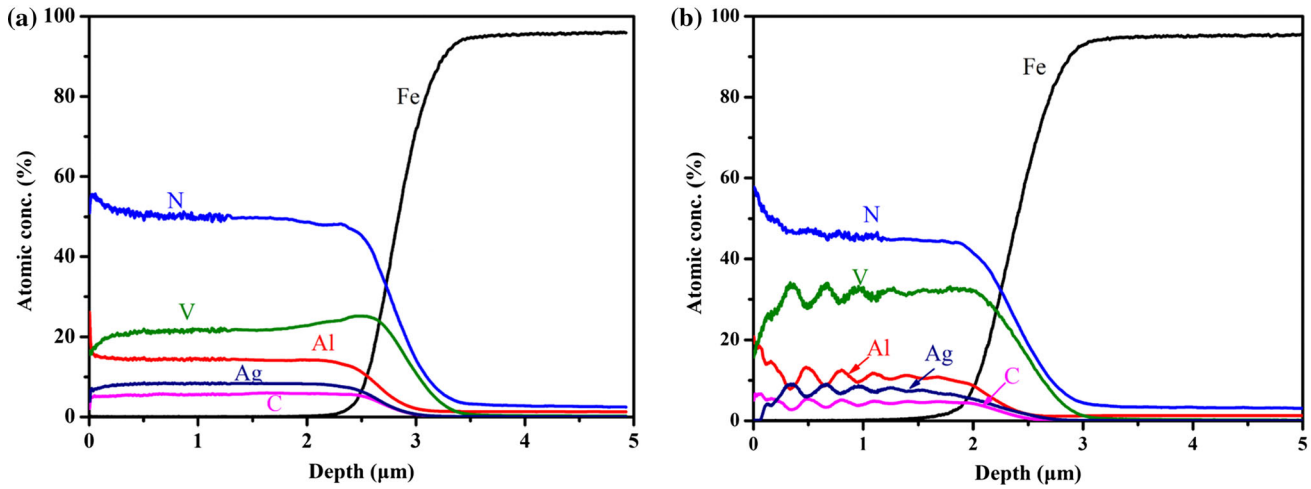

Figure 2 The GDOES elemental depth profiles of VAlCN-Ag composite coating and VAlCN/VN-Ag multilayer coating.

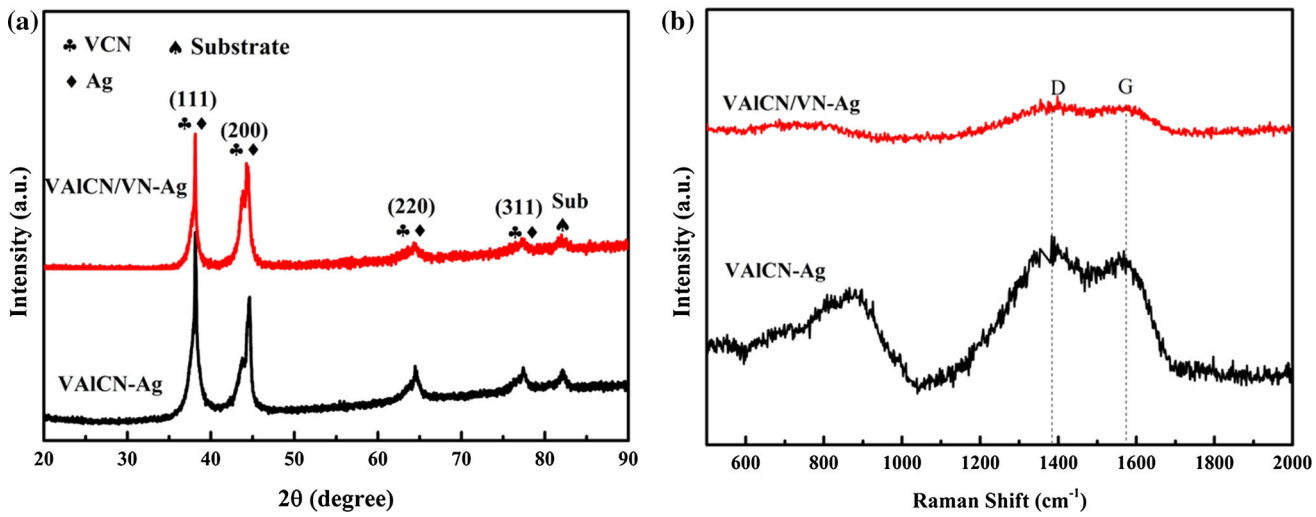

Figure 3 XRD patterns (**a**) and Raman spectrum **b** for the VAlCN-Ag and VAlCN/VN-Ag coatings.

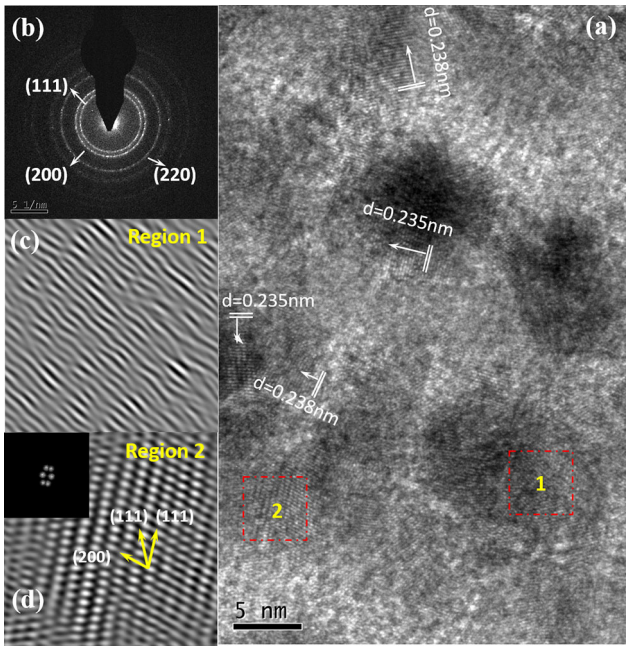

Figure 4 High-resolution TEM images of VAlCN-Ag coating **a** with corresponding SAED patterns (**b**) and inverse Fourier-filtered images **c**, **d** from the region marked by the red box.

Hardness and modulus

The hardness (*H*) and elastic modulus (*E*) of VAlCN-Ag composite and VAlCN/VN-Ag multilayer coatings are shown in Table 1. The VAlCN-Ag coating exhibited a relatively higher hardness of about 22.48 Gpa and high *E* of about 351.84 Gpa when compared with our previous works [31]. Generally speaking, *H* represents the ability to resist the plastic deformation, and *E* is associated with the resistance to elastic deformation. The superior VAlCN-Ag coatings were successfully prepared by altering the number and position of silver targets, indicating a significant improvement of coating properties with a certain addition of silver. The values of $H \sim 27.26$ Gpa and $E \sim 370.15$ GPa are obtained for VAlCN/VN-Ag coating. [37]. Additionally, it displays a relatively high H/E and H^3/E^2 ratio. Usually, the ratio of H/E is the key factor reflecting the wear resistance of coatings [38]. According to the former report, the higher H^3/E^2 ratio indicates a higher fracture toughness of a coating [39]. The multilayer interfaces might provide the VAlCN/VN-Ag coating with higher strength and better toughness. VN/Ag coatings have weak shear strength and good antifriction properties. The interface of the multilayers can suppress the growth of the VN-Ag columnar crystal structure and effectively prevent the dislocation sliding, being responsible for the high hardness of VAlCN/VN-Ag multilayer coating. Moreover, dislocation blocking caused by the coherent strain of different nanocrystals also contributes to the enhancement of hardness [37].

Table1 Nanoindentation results of VAlCN-Ag and VAlCN/VN-Ag coatings

Sample	*H* (GPa)	*E* (Gpa)	*H*/*E*	H^3/E^2 (GPa)
VAlCN-Ag	22.48	351.84	0.064	0.091
VAlCN/VN-Ag	27.26	370.15	0.073	0.147

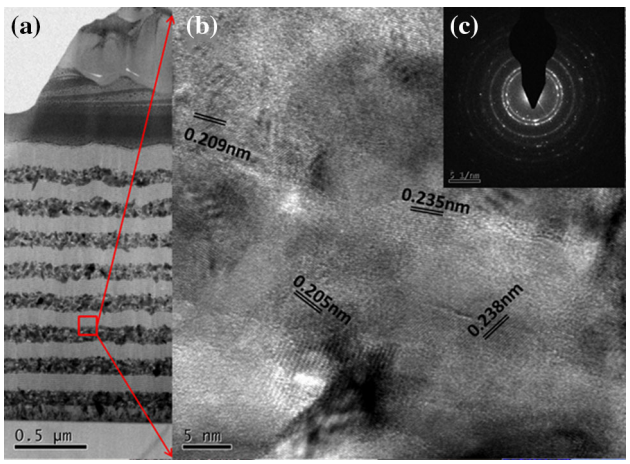

Figure 5 Bright-field (**a**) and high-resolution TEM images **b** with the corresponding STEM of VAlCN/VN-Ag coating (**c**).

Tribological behavior

The average coefficient of friction (COF) measured during tribological testing at different temperatures presented in Fig. 6. It can be seen that the COF values of both coatings intensively depend on the test temperature. The same trend as a function of temperature was observed for all the studied coatings, i.e., the CoF decreased with an increased temperature to 200 °C, then increased when the temperature was further raised to 400 °C, and finally decreased to the lowest COF values at 600 °C. The CoF was found to be very much higher when tribotesting at room temperature as a result of insufficient lubricants. A short but violent running-in stage is visible for VAlCN-Ag coating when the test temperature increases to 400 °C, and subsequently, it enters into a

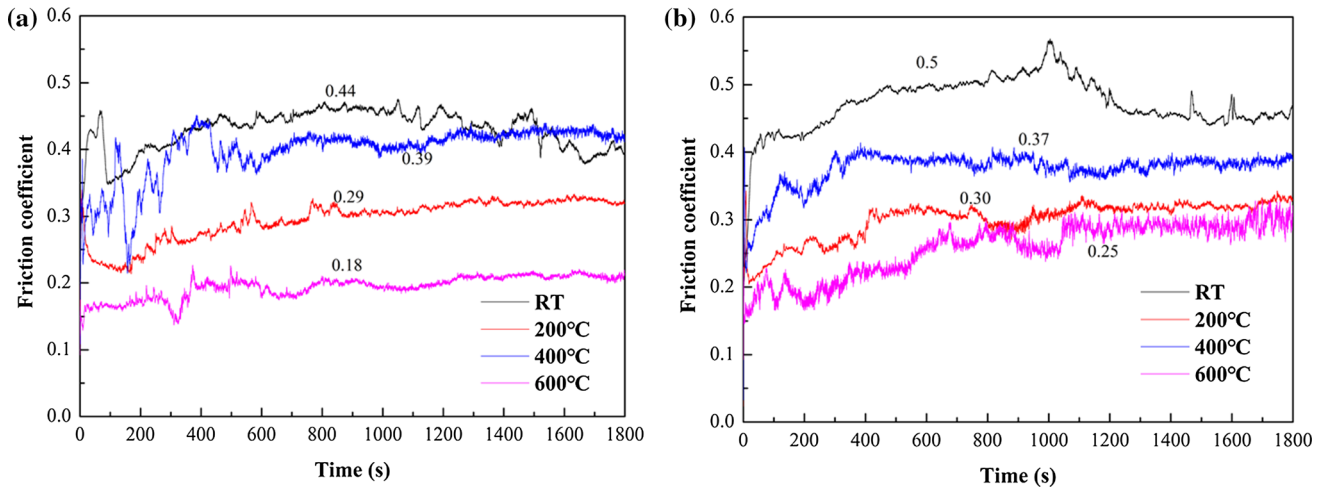

Figure 6 Friction curves of VAlCN-Ag coatings (**a**) and VAlCN/VN-Ag coatings **b** at different temperatures.

relatively smooth stage with an average CoF of ~ 0.39. A similar situation occurs in VAlCN/VN-Ag coating with COF of ~ 0.37. Heated to 600 °C, the VAlCN-Ag and VAlCN/VN-Ag coatings exhibit lowest COF values of ~ 0.18 and ~ 0.25, respectively. This can be ascribed to the positive role of lubricating phases on the worn surface.

Figure 7 gives the wear rate of the VAlCN-Ag composite and VAlCN/VN-Ag multilayer coatings at different temperatures. The calculated wear rates for sets of all coatings present the same pronounced variation along with increasing temperature because of the similar chemical composition. The best wear resistance with the low wear rate of 2.4×10^{-6} mm^3/Nm is found for the VAlCN-Ag coating at room temperature, offering an outstanding combination of high hardness and lubricious soft metals. Meanwhile,

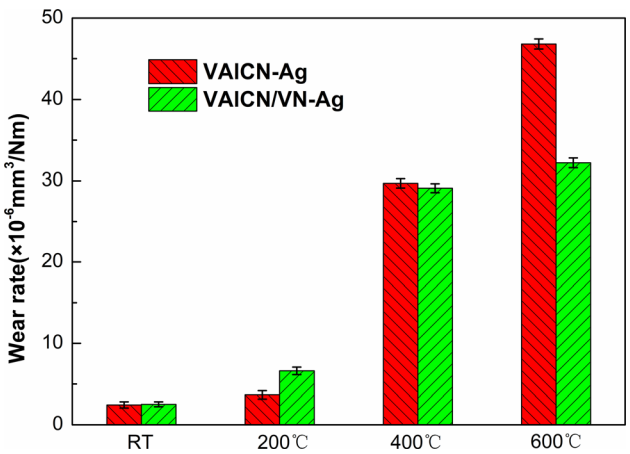

Figure 7 Wear rate for VAlCN-Ag and VAlCN/VN-Ag coatings at different temperatures.

it has higher COF of 0.44, indicating lower energy transmission efficiencies for the coating. The VAlCN-Ag composite coating has a slightly higher wear rate (3.6×10^{-6} mm^3/Nm) when heated to 200 °C, accompanied by decreasing of hardness, resulting in a continuous reduction of the wear resistance. Afterward, the wear resistance increases substantially with the wear rate of 2.9×10^{-5} mm^3/Nm as increasing to 400 °C probably due to the concomitant softening of the coating. It is noted that the wear rate of composite coatings at 600 °C (4.6×10^{-5} mm^3/Nm) is 1.5 times higher than that at 400 °C, while the wear rate of multilayer coatings has no changes than that at 400 °C. Compared with nanocomposite coatings, the VAlCN/VN-Ag multilayer coatings exhibit better wear resistance with elevated temperature.

Figure 8 presents the morphologies of wear tracks of VAlCN-Ag and VAlCN/VN-Ag coatings at 200, 400, and 600 °C. The morphologies of the wear track are distinct at different temperatures. It is noted that the morphologies of the wear track of both the coatings are similar at 200 and 400 °C, but different at 600 °C, which means that different wear mechanisms occur in the two coatings. After sliding friction test under 200 °C, grooves and micro-furrows appear on the worn surface of both the coatings, indicating that the dominant wear mechanism is plastic deformation and abrasive wear. However, the typical characteristics of adhesive wear mechanisms such as adhesion, delamination phenomena, and shallow grooves are present at 400 °C. It is prone to adhesive wear as the softening of coatings and metal oxides on their surfaces under high temperature leads to the increase of

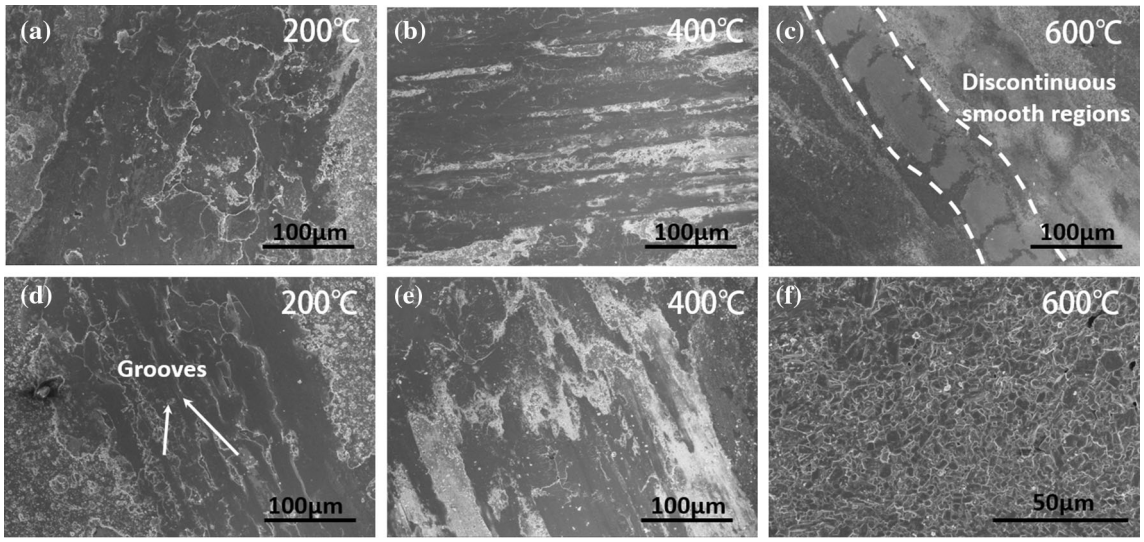

Figure 8 Morphologies of wear tracks for VAlCN-Ag (**a**–**c**) and VAlCN/VN-Ag (**d**–**f**) coatings at different temperatures.

contact area of friction pairs. When the test temperature increases to 600 °C, discontinuous lubrication glaze layer appears on the worn surface of VAlCN-Ag coating, while VAlCN/VN-Ag coating shows a failure pattern of brittle micro-peeling.

To investigate the specific composition of discontinuous glaze regions on the worn surface, the element distribution on the worn surface of VAlCN-Ag composite coating after friction test at 600 °C was inspected, as shown in Fig. 9. A large amount of O elements indicates the occurrence of the oxidation reaction. N and C elements are uniformly distributed on the worn surface. Despite rubbing with the alumina, there are still fewer aluminum elements in the wear area than outside the wear area. This is mainly because Al in the coatings reacts with O at high temperature and forms a dense Al_2O_3 film on the coating surface. However, it is prone to be consumed in the wear area as sliding friction proceeds. A similar distribution of V and Ag elements can be seen. It seems that the metallic oxide and bimetallic oxides ($AgVO_3$ or Ag_3VO_4) form in wear track after the friction test at 600 °C. They act as solid lubricants and make the coating have superior low friction properties.

Subsequently, the Al_2O_3 wear spot was examined after sliding on the surface of VAlCN/VN-Ag coating at 600 °C. As seen in Fig. 10, the distributions of Al and O elements are almost the same. Most of them exist outside the wear spot, corresponding to the composition of alumina ball. The presence of V, Ag, and C elements indicates that the coating material is transferred to the grinding ball during friction, resulting in the formation of metallic oxides and bimetallic oxides.

To verify the origin of low friction friction($\sim$ 0.18), the high-resolution TEM was performed on the worn surface of VAlCN/VN-Ag coating at after the friction test (600 °C). The patterns are shown in Fig. 11. Ag (111) with a lattice spacing of 0.235 and VCN (111) with a lattice spacing of 0.238 can still be found in the wear track as the phase composition in the initial coating. The discovery of Ag (111) illustrates incomplete oxidation of silver when heated to 600 °C. Also, V_2O_5 with a lattice spacing of 0.288 can be found in the wear track and reduce CoF through the shear-prone structure in the sliding contact.

To further determine the relationship between wear products and tribological properties at 600 °C, the Raman spectra on the worn surface for VAlCN-Ag and VAlCN/VN-Ag coatings are presented in Fig. 12. The samples undergo a remarkable chemical reaction. Four distinct oxide phases are detected on both composite and multilayer coatings, including VO_2, V_2O_5, $AgVO_3$, and Ag_3VO_4 [40]. The peaks located at 0–600 cm^{-1} mainly correspond to VO_2 and V_2O_5 phases. Among them, V_2O_5 can provide lubrication due to its shear-prone structure [41–43]. The peaks at 920, 897, 875, and 763 cm^{-1} are ascribed to $AgVO_3$, while the peaks at 783 and 719 cm^{-1} are contributed to Ag_3VO_4 [44]. According to the phase diagram of the V_2O_5–Ag_2O system, the $AgVO_3$ phase has high thermal stability at high temperature [45]. Ag_3VO_4 phase will gradually change into $AgVO_3$

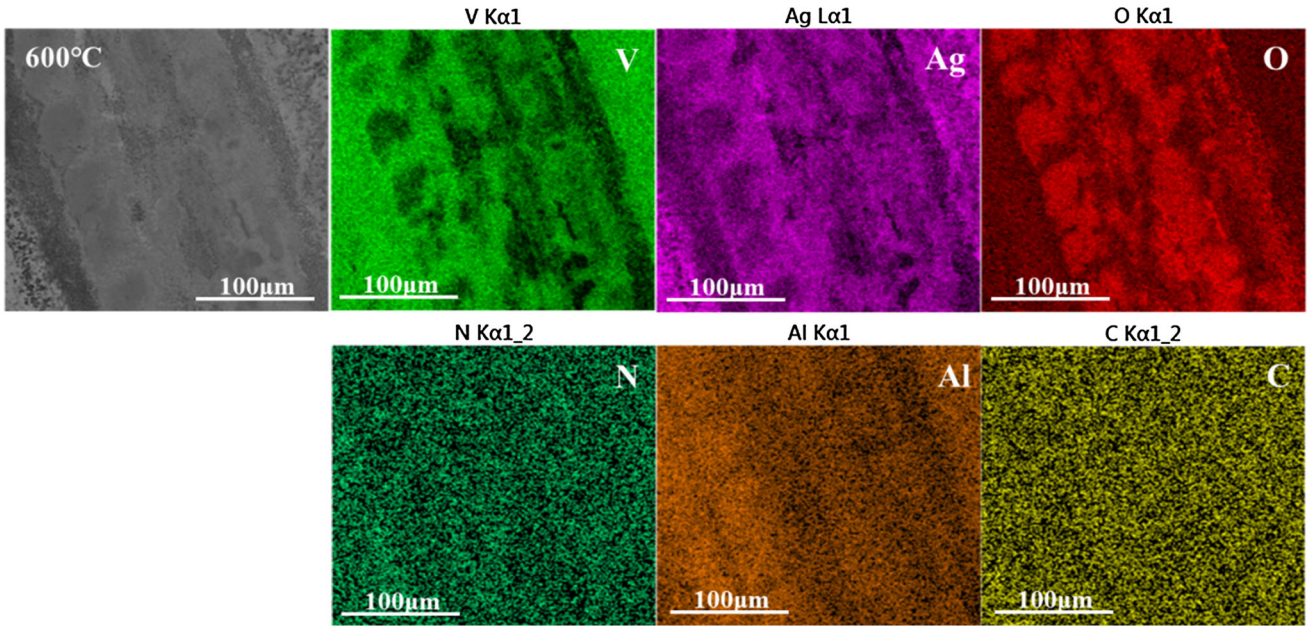

Figure 9 Element distribution maps on the worn surface of VAlCN-Ag coating after friction test at 600 °C.

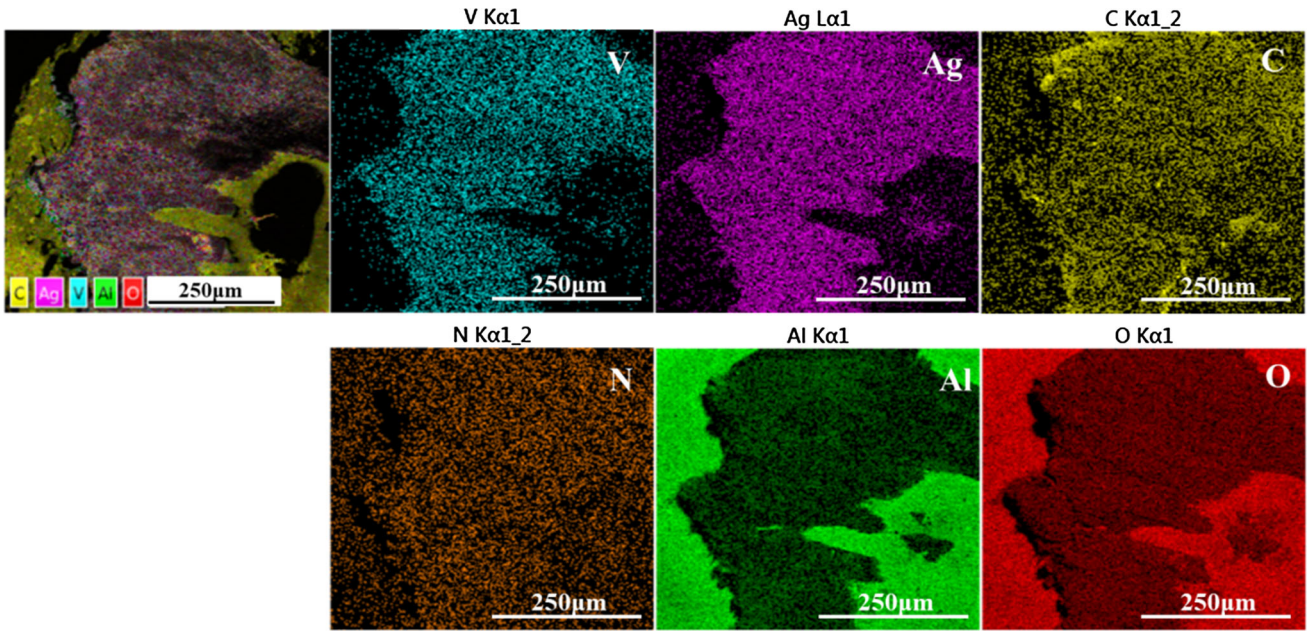

Figure 10 Element distribution maps on the wear scar of Al_2O_3 ball against VAlCN/VN-Ag coating after friction test at 600 °C.

with an increase to temperature. In the process of relative sliding, Ag_3VO_4 is the main initial friction product on the surface of the sample, but the decomposition reaction occurs immediately afterward. Thus, $AgVO_3$ is dominant lubricating phase formed on the worn surface during friction stage. In the crystal structure of $AgVO_3$ phases, Ag–O and Ag–Ag bonds have low shear strength and can be easily slipped under the action of frictional load, resulting in the outstanding lubrication.

The external oxygen participates in tribo-chemical reactions to form metal oxides and bimetallic oxides with good high-temperature lubricity. For the VAlCN/VN-Ag multilayer coating, owing to the existence of multiple interfaces, the permeation of oxygen into the coating can be slowed down. The

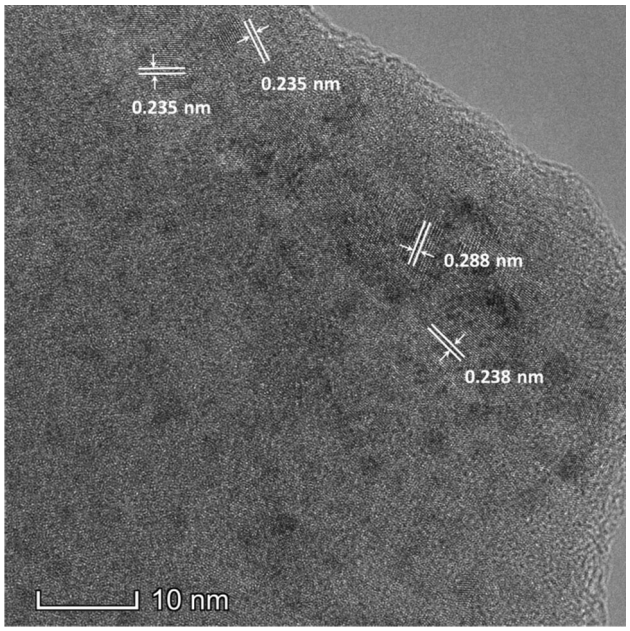

Figure 11 High-resolution image of worn surface of VAlCN/VN-Ag coating after friction test at 600 °C.

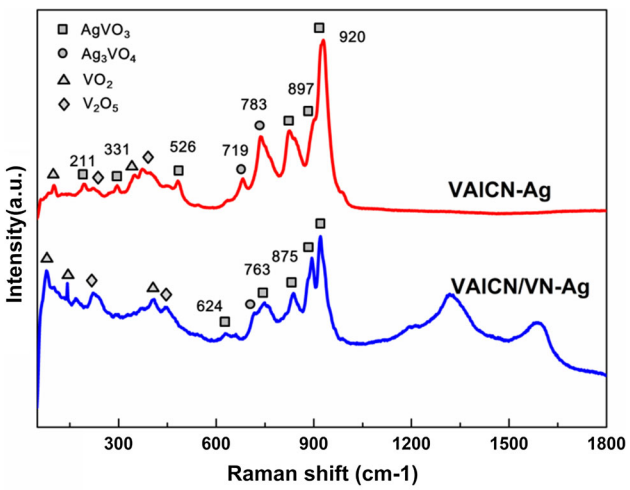

Figure 12 Raman spectra on the worn surface for VAlCN-Ag and VAlCN/VN-Ag coatings after friction test at 600 °C.

formation and loss of the oxide film are balanced dynamically during sliding friction, thus improving the wear resistance of the coatings at high temperature compared with that of composite coatings. Besides, the structure of the coating also affects the oxidation of carbon. There is no carbon peak on the worn surface of the VAlCN-Ag coatings. This result suggests that hybrid C–C bonds in the VAlCN-Ag coating are destroyed by oxidation. Nevertheless, carbon peaks are obvious for VAlCN/VN-Ag multilayer coating, indicating that the oxygen barrier effect of multiple interfaces can protect the carbon phase in the coating.

The Raman spectrum was offered to understand the variation of phase on the worn surface (Fig. 13). It is evident that two peaks around at 1360 (D) and 1580 cm^{-1} (G) can be seen, which indicates that sp^2- and sp^3-hybrized carbon exists in sets of all coatings at RT and 200 °C. It is difficult to form an effective silver lubricating layer on the friction surface at room temperature resulting from the lack of thermal driving force. Thus, the sp^2-hybridized carbon with graphite-like structure plays a major role in lubrication at room temperature. When the temperature rises to 200 °C, silver clusters can diffuse to the coating surface through grain boundary defects under thermal induction, and eventually form a silver-rich lubricating film in the contact sliding area. The peak located at 880 cm^{-1} is attributed to Al_2O_3. At present, the carbon phase can still play a certain role in lubrication. This can be confirmed by the Raman peak of sp2-hybridized carbon on the worn surface at 200 °C. Up to 400 °C, there are many characteristic peaks, located at 229, 297, 412, 508, and 671 cm^{-1}, corresponding to vanadium oxides (VO_2, V_2O_5) phases. The oxidation of carbon and metal elements in the coatings increases when the temperature reaches 400 °C [46, 47]. The sp^2-hybridized carbon with graphite-like structure is essentially difficult to work and usually failure over 300 °C [48, 49]. Only D peaks can be found with increasing temperature to 400 °C, where the position of characteristic peak decreased probably owing to graphitization of the coatings. The low shear strength of oxidation products Ag_2O and V_2O_5 can provide good lubrication. With further increase in temperature to 600 °C, the lowest COF is obtained, which is ascribed to the synergistic lubricant effect derived from stable silver vanadate $AgVO_3$ and V_2O_5 magnéli phases.

To further explain the wear process, wear mechanism diagrams of VAlCN-Ag and VAlCN/VN-Ag coatings after friction test at 600 °C are given in Fig. 14. The structure of a hard nitride matrix is usually compact. Due to the low solid solubility of silver in nitride coating, silver usually exists at the grain boundary defects. Consequently, the silver atoms can diffuse and merge to the surface of the coating through grain boundary defects, and finally form silver particles on the coating surface. In addition, silver on the contact surface has lower chemical

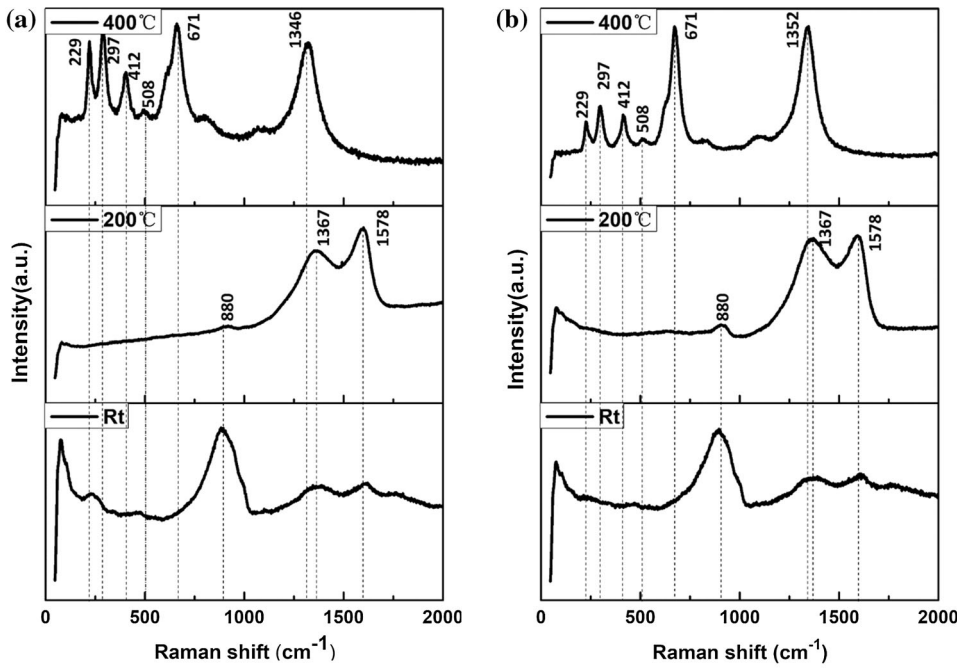

Figure 13 Raman spectrum on the worn surface of VAlCN-Ag and VAlCN/VN-Ag coatings after friction test at room temperature, 200 °C, and 400 °C, respectively.

potential than that embedded in coating, leading to diffusion of more silver atoms to the sliding track, especially at high temperature, thereby forming "transfer film" and providing a constant lubrication.

The silver particles participated in sliding friction will soon be exhausted, resulting in the increase of pinhole and the degradation of mechanical properties of the coatings. The friction coefficient and wear rate are reversed with the increase of temperature, and the service life is significantly cut down. This phenomenon corresponds to VAlCN-Ag composite coatings, where the coating will fail and peel off from substrate as the temperature increases to 650 °C. It is necessary to optimize the diffusion rate of silver to prolong the service life of the coating without changing the friction and wear properties of the original coating. The design of the diffusion barrier in VAlCN/VN-Ag coating optimizes the comprehensive properties of the coating. The multiple interfaces of the VAlCN/VN-Ag coatings can effectively prevent oxygen permeation and silver loss. The silver of the VN-Ag layer can gradually and continuously diffuse to the contact surface to provide longer-term lubrication at 600 °C. The soft-hard alternating interface in multilayer coatings contribute to the fluctuate friction curves while nanocomposite structure of VAlCN-Ag is beneficial to aggregation of silver and formation of lubricating film at worn region.

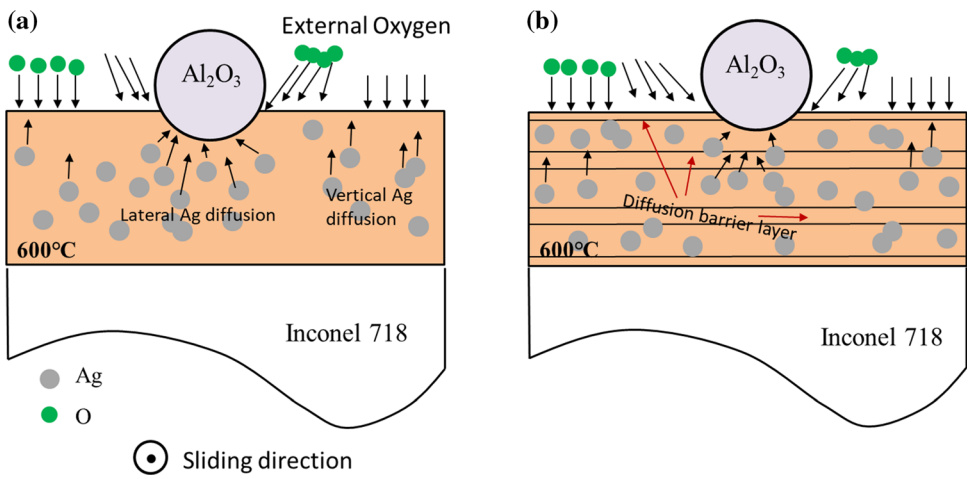

Figure 14 Wear mechanism diagrams of VAlCN-Ag coating (**a**) and VAlCN/VN-Ag coating (**b**).

Hence, the friction coefficient of composite coatings is lower than that of multilayer coatings. In summary, the VAlCN/VN-Ag multilayer coatings have better mechanical, oxidation resistance and wear resistance than VAlCN/Ag composite coating.

Conclusion

The VAlCN-Ag composite and VAlCN/VN-Ag multilayer coatings were deposited by cathodic arc ion plating system in $Ar/N_2/C_2H_2$ atmospheres. Their microstructures, mechanical properties, and tribological properties were characterized. The as-deposited coatings contain vanadium carbonitride, silver, and amorphous carbon phases. The VAlCN-Ag coatings reveal a significantly improved hardness by altering the number and position of targets, compared with previous works. The VAlCN/VN-Ag multilayer coatings exhibit excellent mechanical properties with a higher hardness (27 Gpa) and modulus (370 Gpa). The nanocomposite coatings have the lowest friction coefficient of 0.18 at 600 °C, owing to the synergistic lubricant effect originated from both $AgVO_3$ and V_2O_5 Magnéli phases during tribotesting. The multilayer coatings with higher hardness (27 Gpa) show better oxidation and wear resistance, accompanied with an improving toughness. The multiple interfaces between VN-Ag and VAlCN layers can prevent oxygen diffusion and sustain continuous lubrication at broad temperature (25–600 °C), providing guidance on coating design and potential industrial applications as protective coating under high temperatures (650 °C). There is still a long way to go before it can be employed at higher temperature.

Acknowledgements

The authors are grateful for financial support from the Zhejiang Provincial Natural Science Foundation (Grant No. LR20E050001), National Science and Technology Major Project (2017-VII-0013-0110).

References

[1] Zabinski JS, Sanders JH, Nainaparampil J, Prasad SV (2000) Lubrication using a microstructurally engineered oxide: performance and mechanisms. Tribol Lett 8:103–116

[2] Donnet C, Erdemir A (2004) Solid lubricant coatings: recent developments and future trends. Tribol Lett 17:389–397

[3] Sudagar J, Lian JS, Sha W (2013) Electroless nickel, alloy, composite and nano coatings—a critical review. J Alloys Compd 571:183–204

[4] Zhu SY, Cheng J, Qiao ZH, Yang J (2019) High temperature solid-lubricating materials: a review. Tribol Int 133:206–223

[5] Muratore C, Voevodin AA (2009) Chameleon coatings: adaptive surfaces to reduce friction and wear in extreme environments. Annu Rev Mater Res 39:297–324

[6] Stone D, Liu J, Singh DP, Muratore C, Voevodin AA, Mishra S, Rebholz C, Ge Q, Aouadi SM (2010) Layered atomic structures of double oxides for low shear strength at high temperatures. Scr Mater 62:735–738

[7] Sundgren JE, Birch J, Hakansson G, Hultman L, Helmersson U (1990) Growth, structural characterization and properties of hard and wear-protective layered materials. Thin Solid Films 193:818–831

[8] Kral C, Lengauer W, Rafaja D, Ettmayer P (1998) Critical review on the elastic properties of transition metal carbides, nitrides and carbonitrides. J Alloys Compd 265:215–233

[9] Dellacorte C, Edmonds BJ (1995) Preliminary evaluation of PS300: A new self-lubricating high temperature composite coating for use to 800 °C. NASA/TM-107056

[10] Dellacorte C, Edmonds BJ (2009) NASA PS400: a new temperature solid lubricant coating for high temperature wear applications. NASA/TM-215678

[11] Voevodin AA, Fitz TA, Hu JJ, Zabinski JS (2002) Nanocomposite tribological coatings with "chameleon" surface adaptation. J Vac Sci Technol A: Vac, Surf, Films 20:1434–1444

[12] Baker C, Hu J, Voevodin A (2006) Preparation of Al_2O_3/DLC/Au/MoS_2 chameleon coatings for space and ambient environments. Surf Coat Technol 201:4224–4229

[13] Fateh N, Fontalvo GA, Gassner G, Mitterer C (2007) Influence of high-temperature oxide formation on the tribological behaviour of TiN and VN coatings. Wear 262:1152–1158

[14] Brizuela M, Garcia-Luis A, Braceras I, Onate JI, Sanchez-Lopez JC, Martinez-Martinez D, Lopez-Cartes C, Fernandez A (2005) Magnetron sputtering of Cr(Al)N coatings: mechanical and tribological study. Surf Coat Technol 200:192–197

[15] Ye Y, Jiang Z, Zou Y, Guo S, Zeng X, Yi Z, Yu J, Gui J, Liu T, Chen H (2020) Enhanced anti-wear property of VCN coating in seawater with the optimization of bias voltage. Ceram Int 46:7939–7946

[16] Gassner G, Mayrhofer PH, Kutschej K, Mitterer C, Kathrein M (2004) A new low friction concept for high temperatures:

lubricious oxide formation on sputtered VN coatings. Tribol Lett 17:751–756

[17] Franz R, Mitterer C (2013) Vanadium containing self-adaptive low-friction hard coatings for high-temperature applications: a review. Surf Coat Technol 228:1–13

[18] Glaser A, Surnev S, Netzer FP, Fateh N, Fontalvo GA, Mitterer C (2007) Oxidation of vanadium nitride and titanium nitride coatings. Surf Sci 601:1153–1159

[19] Fateh N, Fontalvo GA, Gassner G, Mitterer C (2007) The beneficial effect of high-temperature oxidation on the tribological behaviour of V and VN coatings. Tribol Lett 28:1–7

[20] Chang YY, Weng SY, Chen CH, Fu FX (2017) High temperature oxidation and cutting performance of AlCrN, TiVN and multilayered AlCrN/TiVN hard coatings. Surf Coat Technol 332:494–503

[21] Gong WJC (2021) Effect of charge voltage on the microstructural, mechanical, and tribological properties of Mo–Cu–V–N nanocomposite coatings. Coatings 11:1595

[22] Zhao H, Yu L, Mu C, Ye F (2016) Structure and properties of Si-implanted VN coatings prepared by RF magnetron sputtering. Mater Charact 117:65–75

[23] Zhu P, Ge F, Li S, Xue Q, Huang F (2013) Microstructure, chemical states, and mechanical properties of magnetron co-sputtered $V_{1-x}Al_xN$ coatings. Surf Coat Technol 232:311–318

[24] Mu YT, Liu M, Zhao YQ (2016) Carbon doping to improve the high temperature tribological properties of VN coating. Tribol Int 97:327–336

[25] Wang Z, Li X, Wang X, Cai S, Ke P, Wang A (2016) Hard yet tough V-Al-C-N nanocomposite coatings: microstructure, mechanical and tribological properties. Surf Coat Technol 304:553–559

[26] Hsieh JH, Chiu CH, Li C, Wu W, Chang SY (2013) Development of anti-wear and anti-bacteria TaN-(Ag, Cu) thin films—a review. Surf Coat Technol 233:159–168

[27] Bondarev AV, Kiryukhantsev-Korneev PV, Sidorenko DA, Shtansky DV (2016) A new insight into hard low friction MoCN-Ag coatings intended for applications in wide temperature range. Mater Des 93:63–72

[28] Basnyat P, Luster B, Kertzman Z, Stadler S, Erdemir A (2007) Mechanical and tribological properties of CrAlN-Ag self-lubricating films. Surf Coat Technol 202:1011–1016

[29] Luster B, Stone D, Singh DP, To Baben M, Schneider JM, Polychronopoulou K, Rebholz C, Kohli P, Aouadi SM (2011) Textured VN coatings with Ag_3VO_4 solid lubricant reservoirs. Surf Coat Technol 206:1932–1935

[30] Bondarev AV, Golizadeh M, Shvyndina NV, Shchetinin IV, Shtansky DV (2017) Microstructure, mechanical, and tribological properties of Ag-free and Ag-doped VCN coatings. Surf Coat Technol 331:77–84

[31] Cai Q, Li SX, Pu JB, Cai ZB, Lu X, Cui QF, Wang LP (2019) Effect of multicomponent doping on the structure and tribological properties of VN-based coatings. J Alloys Compd 806:566–574

[32] Zhang H, Li Z, He W, Liao B, He G, Cao X, Li Y (2018) Damage evolution and mechanism of TiN/Ti multilayer coatings in sand erosion condition. Surf Coat Technol 353:210–220

[33] Pradhaban G, Kuppusami P, Ramachandran D, Viswanathan K, Ramaseshan R (2016) Nanomechanical properties of TiN/ZrN multilayers prepared by pulsed laser deposition. In: Materials today-proceedings, pp 1627–1632

[34] Wang YX, Zhang S (2014) Toward hard yet tough ceramic coatings. Surf Coat Technol 258:1–16

[35] Rao J, Sharma A, Rose T (2018) Titanium aluminium nitride and titanium boride multilayer coatings designed to combat tool wear. Coatings 8:12

[36] Boxman R (1992) Macroparticle contamination in cathodic arc coatings: generation, transport and control. Surf Coat Tech 52:39–50

[37] Zhang J, Wang M, Yang J, Liu Q, Li D (2007) Enhancing mechanical and tribological performance of multilayered CrN/ZrN coatings. Surf Coat Technol 201:5186–5189

[38] Leyland A, Matthews A (2000) On the significance of the H/E ratio in wear control: a nanocomposite coating approach to optimised tribological behaviour. Wear 246:1–11

[39] Chen XJ, Du Y, Chung YW (2019) Commentary on using H/E and H^3/E^2 as proxies for fracture toughness of hard coatings. Thin Solid Films 688:137265

[40] Ningyi Y, Jinhua L, Chenglu L (2002) Valence reduction process from sol–gel V_2O_5 to VO_2 thin films. Appl Surf Sci 191:176–180

[41] Kutschej K, Mayrhofer P, Kathrein M, Polcik P, Mitterer C (2005) Influence of oxide phase formation on the tribological behaviour of Ti–Al–V–N coatings. Surf Coat Technol 200:1731–1737

[42] Tillmann W, Kokalj D, Stangier D, Paulus M, Sternemann C, Tolan M (2018) Investigation on the oxidation behavior of AlCrVxN thin films by means of synchrotron radiation and influence on the high temperature friction. Appl Surf Sci 427:511–521

[43] Tseng C, Hsieh J, Wu W, Chang S, Chang C (2008) Surface and mechanical characterization of TaN–Ag nanocomposite thin films. Thin Solid Films 516:5424–5429

[44] Aouadi SM, Singh DP, Stone D, Polychronopoulou K, Nahif F, Rebholz C, Muratore C, Voevodin AA (2010) Adaptive VN/Ag nanocomposite coatings with lubricious behavior from 25 to 1000 °C. Acta Mater 58:5326–5331

[45] Albrecht TA, Stern CL, Poeppelmeier KR (2007) The $Ag_2O-V_2O_5-HF$ (aq) System and Crystal Structure of α-Ag_3VO_4. Inorg Chem 46:1704–1708

[46] Voevodin AA, Zabinski J (2005) Nanocomposite and nanostructured tribological materials for space applications. Compos Sci Technol 65:741–748

[47] Zhang S, Bui XL, Li X (2006) Thermal stability and oxidation properties of magnetron sputtered diamond-like carbon and its nanocomposite coatings. Diam Relat Mater 15:972–976

[48] Mulligan C, Blanchet T, Gall D (2010) CrN–Ag nanocomposite coatings: tribology at room temperature and during a temperature ramp. Surf Coat Technol 204:1388–1394

[49] Gao H, Otero-de-la-Roza A, Gu J, Stone DA, Aouadi SM, Johnson ER, Martini A (2015) (Ag, Cu)–Ta–O ternaries as high-temperature solid-lubricant coatings. Acs Appl Mater Inter 7:15422–15429